Disclosure of potential conflict of interest: The authors declare that they have no relevant conflicts of interest.

REFERENCES

1. Cosio BG, Mann B, Ito K, Jazrawi E, Barnes PJ, Chung KF, et al. Histone acetylase and deacetylase activity in alveolar macrophages and blood mononocytes in asthma. Am J Respir Crit Care Med 2004;170:141-7.
2. Bhavsar P, Ahmad T, Adcock IM. The role of histone deacetylases in asthma and allergic diseases. J Allergy Clin Immunol 2008;121:580-4.
3. Aoshiba K, Nagai A. Differences in airway remodeling between asthma and chronic obstructive pulmonary disease. Clin Rev Allergy Immunol 2004;27:35-43.
4. Barnes PJ. The cytokine network in asthma and chronic obstructive pulmonary disease. J Clin Invest 2008;118:3546-56.
5. Yamagata T, Mitani K, Oda H, Suzuki T, Honda H, Asai T, et al. Acetylation of GATA-3 affects T-cell survival and homing to secondary lymphoid organs. EMBO J 2000;19:4676-87.
6. Zhu J, Min B, Hu-Li J, Watson CJ, Grinberg A, Wang Q, et al. Conditional deletion of Gata3 shows its essential function in T_H1-T_H2 responses. Nat Immunol 2004;5:1157-65.
7. Kugel S, Mostoslavsky R. Chromatin and beyond: the multitasking roles for SIRT6. Trends Biochem Sci 2014;39:72-81.

Available online June 11, 2016.
http://dx.doi.org/10.1016/j.jaci.2016.05.019

B-cell–specific STAT3 deficiency: Insight into the molecular basis of autosomal-dominant hyper-IgE syndrome

To the Editor:

Autosomal-dominant hyper-IgE syndrome (AD-HIES) is a rare multisystemic primary immunodeficiency disorder characterized by recurrent mucocutaneous candidiasis, *Staphylococcal* abscesses, pneumonia, and extremely high levels of IgE.[1] It is caused by heterozygous loss-of-function mutations in the gene encoding the transcription factor signal transducer and activator of transcription 3 (STAT3). STAT3 acts downstream of many cytokine receptors key to lymphocyte function including those for IL-6, IL-10, and IL-21 and has emerged as a key regulator of multiple lymphocyte lineages including CD4 and CD8 T cells.[1]

AD-HIES is also associated with aberrant B-cell responses including strikingly elevated levels of serum IgE, and specific antibody deficiency.[2] However, the mechanisms underlying these humoral defects remain ill defined. In particular, it is unclear whether the humoral defects observed in AD-HIES stem from a B-cell–intrinsic requirement for STAT3 or are secondary to the action of STAT3 in other cell types such as T follicular helper (Tfh) cells, which are crucial for providing help to B cells for the generation of an effective antibody response. An initial study in mice reported a requirement for B-cell–intrinsic STAT3 function for the generation of normal frequencies of antigen-specific IgG plasma cells.[3] However, patients with AD-HIES also have reduced circulating Tfh-like cells[4] and mice lacking *Stat3* in T cells showed impaired Tfh formation,[5] suggesting that T-cell–specific STAT3 may be more critical for determining the outcome of humoral responses.

We have now sought to further clarify the B-cell–intrinsic *in vivo* requirements for STAT3 during T-cell–dependent B-cell responses using a mouse model (see this article's Methods section in the Online Repository at www.jacionline.org). We generated mice with B-cell-lineage–specific inactivation of *Stat3* ($Stat3^{fl/fl}CD19^{cre/+}$, hereafter referred to as *Stat3*ΔB) and crossed them with SW_{HEL} mice expressing a B-cell receptor (BCR) specific for hen egg lysozyme (HEL). SW_{HEL}.*Stat3*ΔB or SW_{HEL}.Wild-type (WT) B cells were adoptively transferred into WT recipients and the mice then immunized with the low-affinity HEL mutant protein (HEL^{2X}) conjugated to sheep red blood cells (SRBCs) (SRBC-HEL^{2X}). This resulted in a rapid expansion of WT SW_{HEL} cells that peaked at day 5.5 (Fig 1, *A*). The expansion of *Stat3*ΔB cells also peaked at day 5.5 but displayed a dramatic decrease in the magnitude of expansion, which was maintained throughout the time course. This defect was not restricted to a particular B-cell subset as we observed that both WT and *Stat3*ΔB SW_{HEL} donor cells had differentiated into germinal center (GC) B cells and plasmablasts (PBs) at day 5.5 (see Fig E1, *A* and *B*, in this article's Online Repository at www.jacionline.org). However, *Stat3*ΔB donor B cells displayed a slightly skewed differentiation profile with reduced proportions of GC B cells and conversely increased proportions of PBs compared with WT cells (Fig 1, *B*; Fig E1, *A*), suggesting that STAT3 in B cells may play a regulatory role in this process but is not absolutely essential for the differentiation of GC B cells or PBs.

To determine the nature of the expansion defect, we assessed both proliferation and apoptosis. Analysis of bromodeoxyuridine incorporation at day 4.5 revealed no significant difference between *Stat3*ΔB and WT B cells, indicating that the cells have similar levels of proliferation (Fig 1, *C*). In contrast, at day 4.5, *Stat3*ΔB B cells exhibited significantly higher rates of apoptosis (as assessed by Caspase 3 and Annexin V staining) compared with WT cells (Fig 1, *D*; Fig E1, *C*). Collectively, these data suggest that STAT3 signaling in B cells contributes to their optimal expansion by reducing apoptosis. This is consistent with previous reports that STAT3 can regulate expression of Bcl-2 family members[6] and our finding that human STAT3 mutant naive B cells exhibit increased spontaneous apoptosis *in vitro*.[2]

We then determined whether reduced numbers of antigen-specific B cells were associated with a reduction in secreted antibody levels. Over time, recipients of both WT and *Stat3*ΔB SW_{HEL} B cells showed an increase in serum concentrations of HEL-specific IgM, IgG_1, IgG_{2b}, IgG_{2c}, and IgG_3. However, the magnitude of the increase in IgM, IgG_1, IgG_{2b}, and IgG_3 was significantly lower in recipients of *Stat3*ΔB compared with WT SW_{HEL} B cells (Fig 2, *A*; see Fig E2, *A*, in this article's Online Repository at www.jacionline.org). These results recapitulate the finding of Fornek et al[3] of reduced antigen-specific IgG levels; however, we also observed a decrease in IgM levels, indicating a general loss of antigen-specific responses rather than a defect in switching to a specific immunoglobulin isotype. Indeed, we found that class switch recombination to IgG by both PBs and GC B cells was only modestly impaired (Fig E2, *B*) consistent with a complementary, rather than requisite, role for STAT3 in this process. This is also in keeping with previous data that showed only minor defects in switching to IgG *in vitro* by naive B cells from patients with AD-HIES following stimulation with IL-4 and/or IL-21.[2]

Intriguingly, we found that mice that received *Stat3*ΔB SW_{HEL} cells had dramatically increased levels of anti-HEL IgE compared with WT recipients (Fig 2, *B*), mirroring the elevated IgE level observed in patients with AD-HIES. This was also associated with the presence of a substantial proportion of

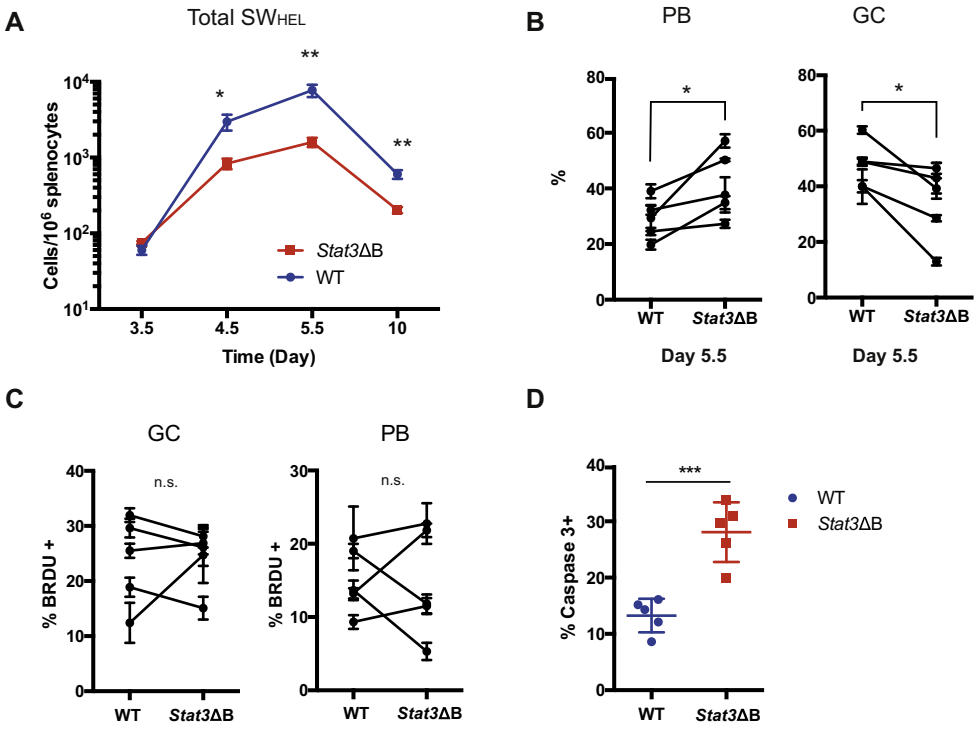

FIG 1. Stat3 deficiency in B cells impairs the expansion of antigen-specific cells. SW_{HEL} WT or *Stat3*ΔB cells were adoptively transferred and recipients immunized with HEL^{2X}-SRBC. **A,** Total SW_{HEL} donor cells (mean ± SEM, 4-5 mice/group, representative of 5 experiments). **B,** Proportion of GC and PBs. **C,** Percentage of HEL-specific cells that incoporporated BrdU in 1 hour, at day 4.5. **D,** Percentage of Caspase3^{+} HEL-binding cells at day 4.5. Fig 1, *B* and *C*, shows paired data (mean ± SEM, 3-5 mice/group) from independent experiments. **D,** Representative of 2 experiments. *BrdU*, Bromodeoxyuridine; *n.s.*, not significant. $*P \leq .05$, $**P \leq .01$, and $***P \leq .001$.

IgE^{+} switched *Stat3*ΔB SW_{HEL} PBs (Fig E2, *C* and *D*). These results demonstrate that STAT3 deficiency drives aberrant switching to, and secretion of, IgE in a B-cell–intrinsic manner. Because HEL^{2X}-SRBC antigen does not stimulate antigen-specific IgE in WT mice, this suggests that STAT3 must act as a negative regulator of IgE switching. This most likely occurs downstream of IL-21 because mice deficient in IL-21 or IL-21R, a key STAT3 activating receptor, also have elevated IgE level.[7] Interestingly, a previous study reported that STAT3-deficient B cells did not have increased IgE secretion in the context of an IgE-inducing immunization (TNP-CGG+ alum),[3] suggesting that in the presence of adjuvants such as alum that strongly promote IgE switching through IL-4[8] the suppressive role of STAT3 may be ablated.

We also determined whether STAT3 deficiency in B cells altered the quality of the antibody response. Affinity maturation is required for the generation of high-quality antibodies and results from preferential selection of higher affinity clones generated by somatic hypermutation (SHM) of the variable region genes of the BCR. At day 10 we found that *Stat3* ΔB GC B cells had reduced affinity maturation as demonstrated by fewer HEL^{3X} binding cells (Fig 2, *C*; Fig E2, *E*). Increased affinity of the SW_{HEL} BCR to HEL^{3X} is associated with the preferential selection for clones that have acquired the Y53D mutation in the immunoglobulin heavy chain.[9] Single-cell SHM analysis of the immunoglobulin heavy-chain variable regions of donor-derived GC B cells at day 10 postimmunization revealed that there was a striking failure of *Stat3*ΔB cells to select for clones bearing the Y53D mutation (22.3% vs 72.6%; Fig 2, *D*) even though *Stat3* ΔB GC B cells acquired mutations at similar rates to WT cells (average mutations/sequence: *Stat3* ΔB 2.2 vs WT 2.8). Thus, although the global process of SHM is unaffected by STAT3 deficiency, B cells require STAT3 for the efficient selection of high-affinity clones.

By using a mouse model to clarify the role of B-cell–intrinsic STAT3 in the context of a dynamic immune response to a specific and well-defined T-dependent antigen, our results reveal that deficiency of STAT3 in B cells alone recapitulates the key humoral defects of AD-HIES of aberrantly elevated IgE level, and impaired specific antibody production. Furthermore, these data provide new insight into the mechanisms underlying the impaired specific antibody production. First, there is impairment in the clonal expansion of naive antigen-specific B cells; second, there is impaired positive selection of high-affinity matured B-cell clones, resulting in accumulation of low-affinity binding cells; third, there is a modest but significant reduction in class-switching of antigen-specific cells. We propose that these combined quantitative and qualitative impairments act in summation to result in a defective antigen-specific response characterized by low serum levels of class-switched antigen-specific antibody that is seen in AD-HIES. Collectively, these findings reveal not only the mechanism underlying the humoral impairments in AD-HIES but also B-cell–intrinsic STAT3 signaling as a key regulator of fate decisions during antibody responses.

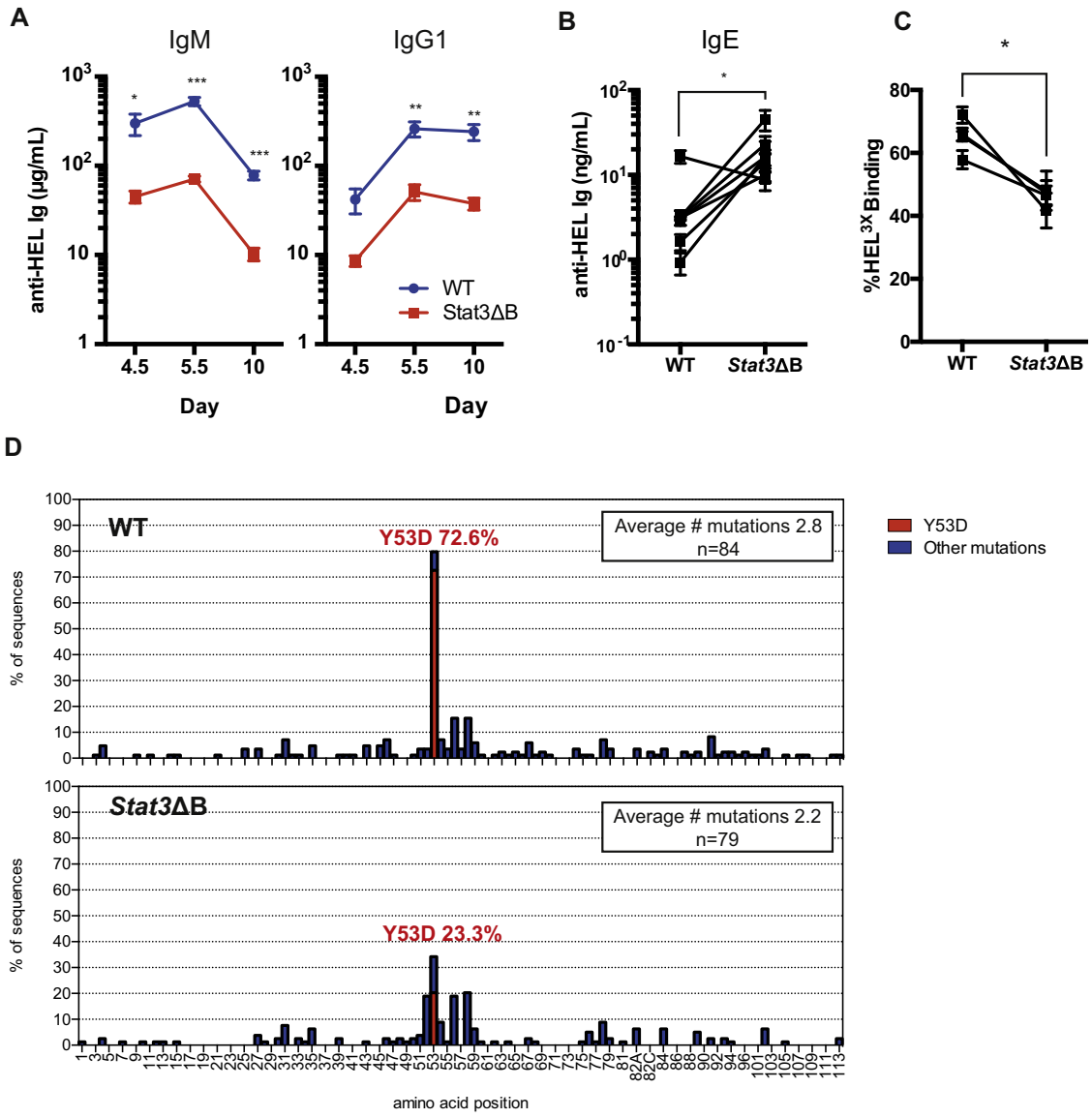

FIG 2. Stat3 deficiency in B cells results in reduced serum antigen-specific antibody levels and impaired affinity maturation. WT or *Stat3*ΔB SW_{HEL} cells were adoptively transferred and recipients immunized with HEL^{2X}-SRBC. Serum concentration of anti-HEL **(A)** IgM and IgG_1 (mean ± SEM, 4-5 mice/group, representative of 4 experiments) and **(B)** IgE (day 5.5). **C,** Percentage of high-affinity cells in IgG_1^+ SW_{HEL} GC B cells at day 10. Fig 2, *B* and *C*, Paired data from independent experiments (mean ± SEM, 2-5 mice/group). **D,** Somatic hypermutation (SHM) analysis of donor GC B cells at day 10. Percentage of clones with Y53D (*red* bars) or other (*blue* bars) mutations (combined data from 2 experiments). $*P \leq .05$, $**P \leq .01$, and $***P \leq .001$.

We thank Kiyoshi Takeda for making the *Stat3*$^{fl/fl}$ mice available for this study and Marc Pellegrini for providing us with these mice; the staff of the Garvan Institute Biological Testing Facility for animal husbandry; the Garvan Flow Facility for cell sorting; and the Garvan Molecular Genetic facility for gene sequencing.

Alisa Kane, MB, BS[a,b]
Anthony Lau[a,c]
Robert Brink, PhD[a,b]
Stuart G. Tangye, PhD[a,b]
Elissa K. Deenick, PhD[a,b]

From [a]the Immunology Division, Garvan Institute of Medical Research, Darlinghurst, Australia; [b]St Vincent's Clinical School, UNSW Australia, Darlinghurst, Australia; and [c]the University of Bath, Bath, United Kingdom. E-mail: e.deenick@garvan.org.au.

This work was supported by grants awarded by the National Health and Medical Research Council (NHMRC) of Australia (grant nos. 1016953, 1066694, and 1027400 to S.G.T. and E.K.D.). A.K. is supported by a Postgraduate scholarship (1038881) and R.B. and S.G.T. by Principal Research Fellowships (1042925, 1105877) from the NHMRC.

Disclosure of potential conflict of interest: A. Kane has received research support from the National Health and Medical Research Council (NHMRC). R. Brink has received research support from NHMRC Australia. S. G. Tangye has received research support from the NHMRC; has received travel support as an invited speaker at Keystone Symposia; has received consultancy fees from Eli Lilly; and has provided expert witness testimony in a patent dispute. E. K. Deenick has received research support from the NHMRC and has received travel support from Baxalta. A. Lau declares that he has no relevant conflicts of interest.

REFERENCES

1. Kane A, Deenick EK, Ma CS, Cook MC, Uzel G, Tangye SG. STAT3 is a central regulator of lymphocyte differentiation and function. Curr Opin Immunol 2014; 28C:49-57.

2. Avery DT, Deenick EK, Ma CS, Suryani S, Simpson N, Chew GY, et al. B cell-intrinsic signaling through IL-21 receptor and STAT3 is required for establishing long-lived antibody responses in humans. J Exp Med 2010;207:155-71.
3. Fornek JL, Tygrett LT, Waldschmidt TJ, Poli V, Rickert RC, Kansas GS. Critical role for Stat3 in T-dependent terminal differentiation of IgG B cells. Blood 2005;107:1085-91.
4. Ma CS, Avery DT, Chan A, Batten M, Bustamante J, Boisson-Dupuis S, et al. Functional STAT3 deficiency compromises the generation of human T follicular helper cells. Blood 2012;119:3997-4008.
5. Ray JP, Marshall HD, Laidlaw BJ, Staron MM, Kaech SM, Craft J. Transcription factor STAT3 and type I interferons are corepressive insulators for differentiation of follicular helper and T helper 1 cells. Immunity 2014;40:307-9.
6. Durant L, Watford WT, Ramos HL, Laurence A, Vahedi G, Wei L, et al. Diverse targets of the transcription factor STAT3 contribute to T cell pathogenicity and homeostasis. Immunity 2010;32:605-15.
7. Ozaki K. A critical role for IL-21 in regulating immunoglobulin production. Science 2002;298:1630-4.
8. Lindblad EB. Aluminium compounds for use in vaccines. Immunol Cell Biol 2004;82:497-505.
9. Phan TG, Paus D, Chan TD, Turner ML, Nutt SL, Basten A, et al. High affinity germinal center B cells are actively selected into the plasma cell compartment. J Exp Med 2006;203:2419-24.

Available online June 11, 2016.
http://dx.doi.org/10.1016/j.jaci.2016.05.018

The potential for repositioning antithyroid agents as antiasthma drugs

To the Editor:

Bronchial asthma is a common disease in which type 2 immunity is dominant.[1] Based on this immunological background, various antiasthma drugs targeting type 2 immune mediators, such as IL-4, IL-5, IL-13, and CRTH2, are now under development.[2] However, to develop novel drugs, particularly biologics, huge investments of time and money are required and safety risks are involved. *Drug repositioning*, which is the process of finding new therapeutic indications for existing drugs, is highly desirable as an alternative strategy.[3,4] However, to our knowledge, there has been no instance of drug repositioning in bronchial asthma.

Airway peroxidase functions as a potent defense system against microbes by producing biocidal compounds, including hypothiocyanite ($OSCN^-$), together with hydrogen peroxide generated by Duox1 and Duox2, which are members of the Nox/Duox family.[5,6] Three heme peroxidases—myeloperoxidase (MPO), eosinophil peroxidase (EPX), and lactoperoxidase (LPO) (expressed at neutrophils, eosinophils, and epithelial cells, respectively)—are involved in this system in the lung tissues. In contrast, the deleterious effects of the airway peroxidase system in bronchial asthma remain undetermined. To define the pathological roles of peroxidase in bronchial asthma, we applied heme peroxidase inhibitors widely used as antithyroid agents to a mouse model of allergic airway inflammation. We found that these agents efficiently inhibited allergic airway inflammation. These results suggest that antithyroid agents can be repositioned as antiasthma drugs.

We first examined the expression of 3 airway peroxidase genes in a mouse model of allergic airway inflammation. The pulmonary expression of all 3 heme peroxidases (*Mpo*, *Epx*, and *Lpo*) was significantly upregulated in response to an allergen challenge (Fig 1, *A*). The peroxidase activities were also enhanced in the bronchoalveolar lavage fluids (BALFs) of allergen-challenged mice (Fig 1, *B*). We then collected bronchial biopsy samples from 10 patients with asthma (see Table E1 in this article's Online Repository at www.jacionline.org) to determine whether the expression of the heme peroxidases was also enhanced in the bronchial tissues of patients with asthma. The peroxidase activities and the expression levels of *LPO* were not statistically enhanced. No expression of *EPX* or *MPO* was detected or was invariant between the patients and normal donors in contrast to the mouse analyses (Fig 1, *C*, data not shown). However, some patients showed distinctly high peroxidase activities and *LPO* expression. This may be due to the background (steps 2-4 according to the GINA2014 criteria), effects of the treatment for the patients (under good control of inhaled corticosteroids [ICSs]), and/or heterogeneity among patients with asthma regarding airway peroxidase expression. These results suggest the involvement of the airway peroxidase system at least in the mouse model of allergic airway inflammation and possibly in some patients with asthma.

We applied the heme peroxidase inhibitors to examine the role of the airway peroxidase system in allergic airway inflammation. The approach we took to understand the role of this production system during allergic inflammatory responses involved inhibiting all peroxidase-mediated events in the lung because no inhibitors specific for *LPO*, *MPO*, or *EPX* have been developed. We examined the effects of 2-mercapto-1-methylimidazole (methimazole) and 6-propyl-2-thiouracil (PTU), which are agents that inhibit all peroxidases and are widely used as antithyroid agents targeting thyroid peroxidase. For the experiments of methimazole or PTU ingestion, 0.2 mg/mL of methimazole (Wako Pure Chemical Industries, Osaka, Japan) or 0.5 mg/mL of PTU (Sigma-Aldrich, St Louis, Mo) in drinking water was administered orally every day for the indicated times. We adopted 2 protocols of methimazole administration, a long and a short administration strategy (Met-L and Met-S, respectively) (Fig 2, *A*). Methimazole was administered orally every day from the start of sensitization (day 0) in the long administration and from 2 days before the start of the allergen airway challenge (day 20) in the short administration.

The parameters of ovalbumin (OVA)-induced airway inflammation (ie, airway hyperresponsiveness [AHR], infiltration of inflammatory cells in BALF, and histological changes) were completely inhibited in the long administration and less so (yet significantly) in the short administration (Fig 2, *B-D*). The use of another peroxidase-inhibiting antithyroid agent, PTU, showed effects similar to but smaller than those of methimazole. Nonetheless, these effects showed a statistically significant improvement in AHR at the dosages used in this experiment (0.2 mg/mL of methimazole vs 0.5 mg/mL of PTU) (see Fig E1 in this article's Online Repository at www.jacionline.org). These results strongly suggest that heme peroxidase activities are critical for the setting of allergic airway inflammation in the model mice.

The Met-L decreased free T4 in serum by inhibiting thyroid peroxidase (1.32 ± 0.14 ng/dL vs 2.0 ± 0.27 ng/dL; $P < .001$) (see Fig E2 in this article's Online Repository at www.jacionline.org). We complemented the thyroid function by administering thyroxine to exclude the possibility that the inhibition of airway inflammation by methimazole was due to impaired thyroid function; however, administering thyroxine had no effect on airway responsiveness (see Fig E3 in this article's Online Repository at www.jacionline.org).

METHODS

Mice

Donor mice were generated by crossing *Stat3*$^{fl/fl}$ mice,[E1] on the C57BL/6 (CD45.2) background, with CD19^{cre} mice[E2] to generate *Stat3*$^{fl/fl}$ CD19$^{cre/+}$ mice (*Stat3*ΔB). These were then crossed with SW$_{HEL}$ mice[E3] to generate SW$_{HEL}$.*Stat3*ΔB. Control SW$_{HEL}$.WT mice were *Stat3*$^{+/+}$ CD19$^{cre/+}$ or *Stat3*$^{fl/fl}$ CD19$^{+/+}$. Donor cells were adoptively transferred into C57Bl/6 (CD45.1 congenic) mice purchased from either the Australian Resources Centre or Australian BioResources. Mice were bred and housed in specific pathogen-free conditions in the Garvan Institute Biological Testing Facility or Australian BioResources. All experiments were approved by the Garvan Institute-St Vincent's Animal Ethics Committee.

HEL proteins

Recombinant HEL proteins (HEL^{2X} and HEL^{3X}) were produced as previously described.[E4] HEL^{WT} was purchased from Sigma-Aldrich (St Louis, Mo).

SW$_{HEL}$ adoptive transfers

Adoptive transfer and immunization has been described previously.[E4] In brief, donor SW$_{HEL}$ *Stat3*ΔB or WT spleen cells containing 3×10^4 HEL-binding B cells were injected intravenously into CD45.1 congenic C57BL/6 recipient mice along with 2×10^8 SRBCs conjugated to HEL^{2X}. The conjugation method has been previously described.[E5] Spleens and sera were harvested and analyzed at the time points described. SW$_{HEL}$ cells were identified as CD45.2$^+$CD45.1$^-$HEL$^+$B220$^+$.

mAb and reagents for flow cytometry

The following were purchased from BD Biosciences (Franklin Lakes, NJ): anti-CD45R/B220 phycoerythrin, anti-IgG$_1$ biotin (A85-1), anti-IgM biotin, anti-CD16/CD32 Fc block (2.4G2), anti-CD45.1 biotin (A20), SA-PeCy7, IgE fluorescein isothiocyanate (FITC) (R25-72), anti-CD45.2 FITC (104), anti-CD45R/B220 PB (RA3-6B2), SA BV421, anti-Caspase 3 FITC.

The following were purchased from eBiosciences (San Diego, Calif): anti-CD38 FITC, anti-CD45.1 PerCP-Cy5.5 (104), anti-CD45.2 PE-Cy7 (A20). The following was purchased from Invitrogen (Waltham, Mass): SA-PB.

Flow cytometry

Spleens of recipient mice were harvested at the indicated time points, prepared, and stained for flow cytometry as previously described.[E6,E7] Annexin V staining was performed as previously described.[E6] Caspase 3 staining was performed on fixed and permeablized cells where cells were first stained for surface markers, then fixed with BD Cytofix/Cytoperm. Cells were then washed with BD Perm/Wash buffer, blocked with 5% normal mouse serum (Jackson ImmunoResearch Laboratories, West Grove, Pa), and then stained with anti-Caspase 3 FITC. Data were acquired on FACSCantoI, FACSCantoII, or BD LSR II. Single-cell sorting was performed on the FACSAria. Acquisition and analysis has been previously described.[E6] Approximately 2.0×10^6 to 5.0×10^6 events were collected per sample. All data are representative of 2 or more experiments as indicated.

ELISA

Anti-HEL antibody levels of the various immunoglobulin subclasses in the sera of recipient mice were analyzed by ELISA as previously described.[E3,E5] In brief, 96-well ELISA plates (Nunc, Waltham, Mass) were coated with HEL (Sigma-Aldrich) and bound serum immunoglobulin was detected using immunoglobulin heavy-chain isotype-specific antibody purchased from BD Biosciences: anti-IgG$_1$ biotin (A85-1), anti-IgG$_{2a}$/c biotin (R19-15), anti-IgG$_{2b}$ biotin (R12-3), anti-IgG$_3$ biotin (R40-82), anti-IgM biotin (R6-60.2). IgE ELISAs were performed as described.[E7] In brief, plates were coated with anti-IgE (R35-72), followed by incubation of serum samples. Bound anti–HEL-IgE was detected by biotinyated HEL-WT. Immunoglobulin levels for each class were quantified against rHyHEL10 standards.[E3,E5]

BrdU Labeling

Mice were injected intravenously with 2 mg of BrdU (in 200 μL of PBS) 60 minutes before sacrifice. Spleens were stained with surface molecules, and then fixed, permeablized, and stained with anti-BrdU FITC using the BrdU flow Kit (BD Biosciences) according to the manufacturer's instructions.

Single-cell sorting and SHM analysis

Recipient spleens were prepared and stained as described for flow cytomtery. Donor-derived IgG$_1$-switched GCs were identified using anti-CD45.2 PeCy7, anti-CD45.2 PerCp Cy5.5, anti-B220 PE, anti-CD38 FITC, anti–IgG$_1$-biotin, and SA-PB. Single cells (donor-derived GC B cells; CD45.2$^+$CD45.1$^-$B220$^+$CD38^{lo}IgG1$^+$) were sorted using FACSAria (BD Biosciences). The variable region exon of the SW$_{HEL}$ immunoglobulin (HyHEL10) heavy-chain regions was amplified by PCR and sequenced as previously described.[E4] The final product was sequenced by Garvan Molecular Genetics and analyzed.

Statistical analysis

Data were analyzed using Graphpad Prism (GraphPad Software, La Jolla, Calif) software. An unpaired *t* test was performed to compare 2 groups within a single experiment. A paired *t* test was used to analyze the combined data from several replicate experiments, except for analysis of Annexin V staining and IgE staining, where the ratio paired *t* test was used, and for IgE ELISA, where the Wilcoxon matched pairs signed rank test was used ($*P \leq .05$; $**P \leq .01$; $***P \leq .001$).

REFERENCES

E1. Takeda K, Noguchi K, Shi W, Tanaka T, Matsumoto M, Yoshida N, et al. Targeted disruption of the mouse Stat3 gene leads to early embryonic lethality. Proc Natl Acad Sci U S A 1997;94:3801-4.

E2. Rickert RC, Roes J, Rajewsky K. B lymphocyte-specific, Cre-mediated mutagenesis in mice. Nucleic Acids Res 1997;25:1317-8.

E3. Phan TG, Amesbury M, Gardam S, Crosbie J, Hasbold J, Hodgkin PD, et al. B cell receptor-independent stimuli trigger immunoglobulin (Ig) class switch recombination and production of IgG autoantibodies by anergic self-reactive B cells. J Exp Med 2003;197:845-60.

E4. Paus D, Phan TG, Chan TD, Gardam S, Basten A, Brink R. Antigen recognition strength regulates the choice between extrafollicular plasma cell and germinal center B cell differentiation. J Exp Med 2006;203:1081-91.

E5. Phan TG, Gardam S, Basten A, Brink R. Altered migration, recruitment, and somatic hypermutation in the early response of marginal zone B cells to T cell-dependent antigen. J Immunol 2005;174:4567-78.

E6. Chan TD, Gatto D, Wood K, Camidge T, Basten A, Brink R. Antigen affinity controls rapid T-dependent antibody production by driving the expansion rather than the differentiation or extrafollicular migration of early plasmablasts. J Immunol 2009;183:3139-49.

E7. Butt D, Chan TD, Bourne K, Hermes JR, Nguyen A, Statham A, et al. FAS inactivation releases unconventional germinal center B cells that escape antigen control and drive IgE and autoantibody production. Immunity 2015;42:890-902.

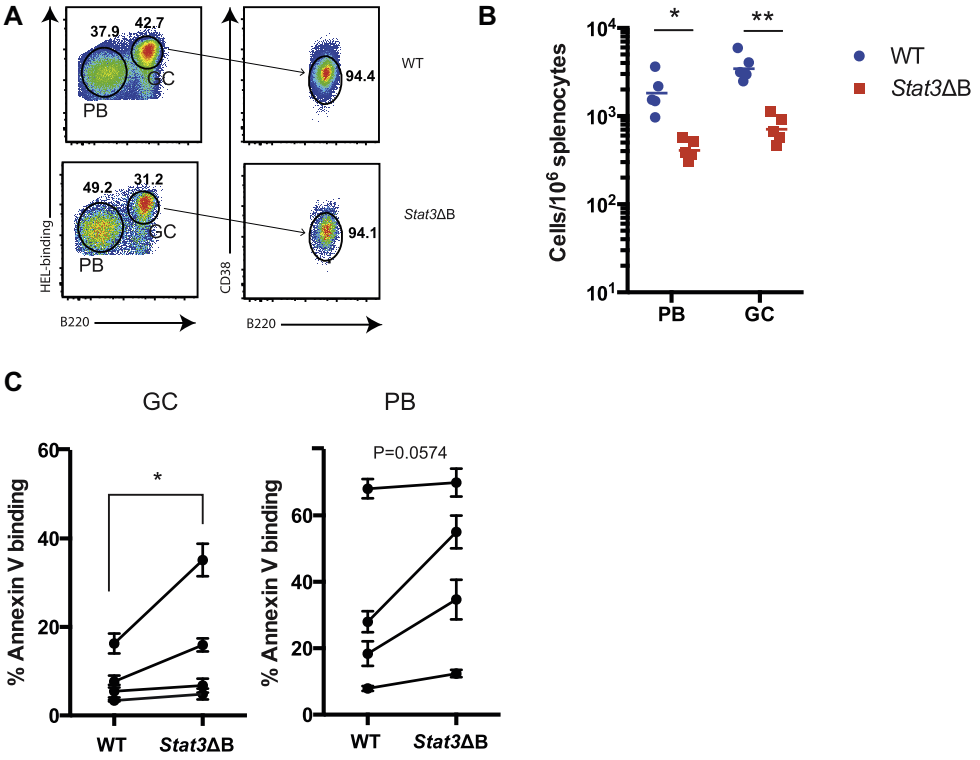

FIG E1. Stat3 deficiency in B cells impairs the expansion of antigen-specific cells. SW_{HEL} transgenic WT or *Stat3*ΔB splenocytes were adoptively transferred and recipients immunized with HEL^{2X}-SRBC. **A,** Cells were stained for B220 and HEL binding and the proportion of $B220^{hi}HEL^{hi}CD38^{lo}$ GC and $B220^{lo}HEL^{lo}$ PBs quantified. Flow cytometry plots show representative staining. **B,** Total number of HEL-specific donor cells per million splenocytes. Each symbol represents a single mouse (line gives mean). Data are representative of 5 independent experiments. Unpaired *t* test (*$P \leq .05$; **$P \leq .01$). **C,** The % of $AnnexinV^{+}$ HEL-binding cells was determined. Plots show paired data from 4 independent experiments. Points represent mean ± SEM (3-5 mice/group).

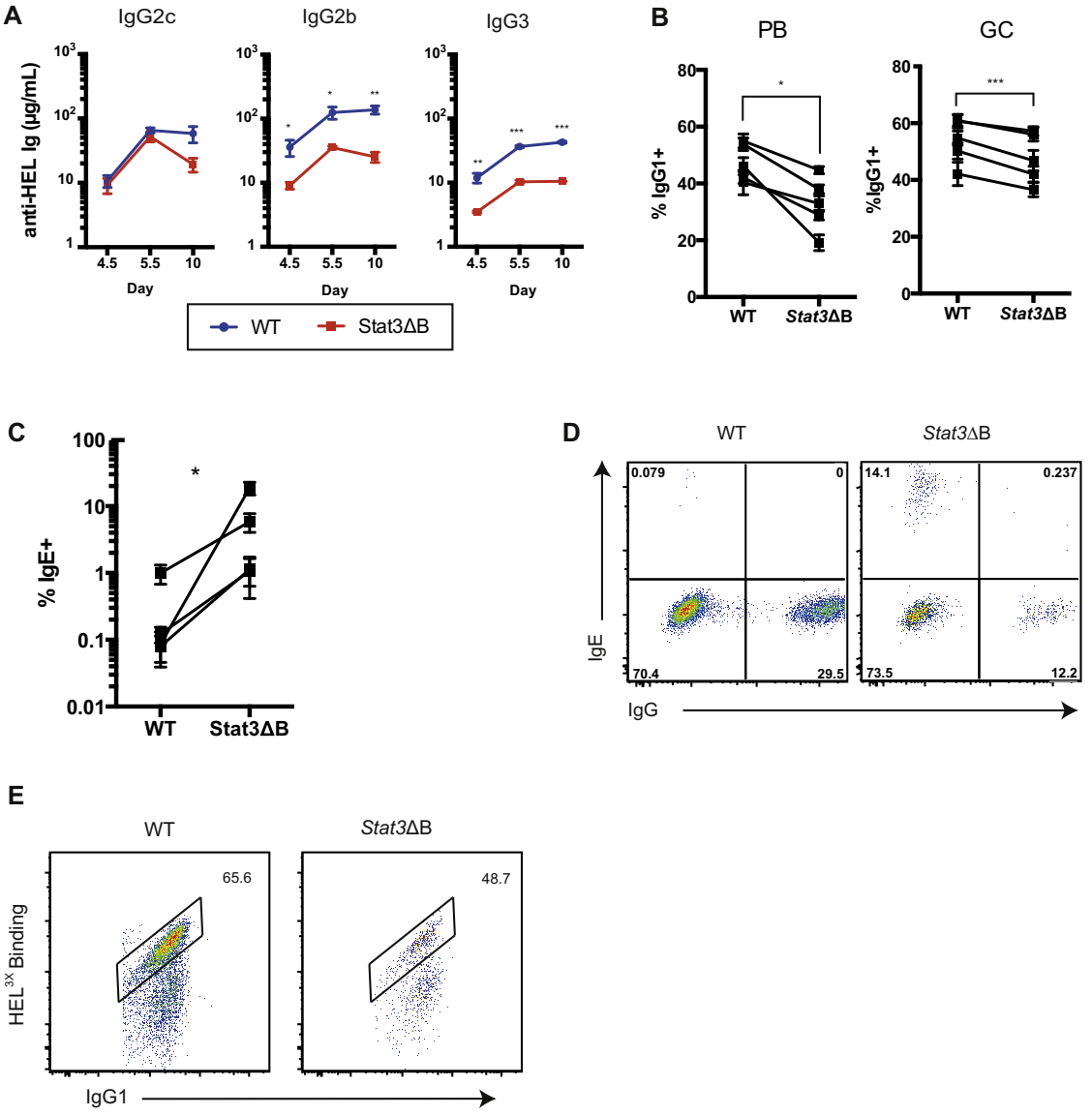

FIG E2. Stat3 deficiency in B cells results in reduced serum antigen-specific antibody levels and impaired affinity maturation. **A,** WT or *Stat3*ΔB SW_{HEL} splenocytes were adoptively transferred and recipients immunized with HEL^{2X}- SRBC. Serum was collected at day 4.5, 5.5, and 10 and analyzed by ELISA for the presence of anti-HEL antibody of IgG_{2c}, IgG_{2b}, and IgG_3 isotypes. Plots represent mean ± SEM of 4 to 5 mice/group and are representative of 3 to 4 independent experiments. **B,** Percentage of IgG_1^+ cells in the PB and GC populations at day 5.5. Graph shows paired data from independent experiments, and plots represent mean ± SEM (4-5 mice/group). Paired *t* test (**P* ≤ .05; ***P* < .01; ****P* ≤ .001). **C** and **D,** Cells were stained for intracellular IgE and IgG_1 expression at day 5.5. Graph (Fig E2, *C*) shows paired data from independent experiments, and plots represent mean ± SEM (5 mice/group). Fig E2, *D,* Flow cytometry plots show concatenated data from 5 mice per group gated on donor PBs ($CD45.2^+CD45.1^-B220^{lo}HEL^{hi}$), representative of 4 independent experiments. **E,** Splenocytes from recipient 10 days after immunization were stained with HEL^{3X} to identify high-affinity cells. Representative flow cytometry plots showing donor SW_{HEL} GC B cells ($CD45.2^+CD45.1^-B220^+CD38^{lo}$; concatenated data from 5 mice).